Development and First Test of the 15 T Nb_3Sn Dipole Demonstrator MDPCT1

A.V. Zlobin, I. Novitski, E. Barzi, V.V. Kashikhin, J. Carmichael, S. Caspi, G. Chlachidze, S. Krave, C. Orozco, D. Schoerling, S. Stoynev, D. Tommasini, D. Turrioni

***Abstract*— Fermilab in the framework of the U.S. Magnet Development Program (MDP) has developed a Nb_3Sn dipole demonstrator for a post-LHC hadron collider. The magnet uses 60-mm aperture 4-layer shell-type graded coils. The cable in the two innermost layers has 28 strands 1.0 mm in diameter and the cable in the two outermost layers has 40 strands 0.7 mm in diameter. An innovative mechanical structure based on aluminum I-clamps and a thick stainless steel skin is used to preload Nb_3Sn coils and support large Lorentz forces. The maximum field for this magnet is limited by 15 T due to mechanical considerations. The first magnet assembly was done with lower coil pre-load to achieve 14 T and minimize the risk of coil damage during assembly. This paper describes the magnet design and the details of its assembly procedure, and reports the results of its cold tests.**

***Index Terms*— coil stress, dipole magnet, mechanical structure, Nb_3Sn superconductor, Rutherford cable, training**

I. Introduction

FERMILAB, in the framework of the U.S. Magnet Development Program (MDP), has developed a Nb_3Sn dipole demonstrator for a post-LHC very high energy hadron collider. The main objectives of this work are demonstration of the field level, suitable for a future hadron collider, and study of the high-field Nb_3Sn magnet behavior, including quench performance, operation margins, field quality, and quench protection.

The magnet design concept uses optimized 4-layer shell-type coils and a cold iron yoke [1]. An innovative mechanical structure based on strong aluminum I-clamps and thick stainless-steel skin [2] or aluminum shell [3] was developed to preload brittle Nb_3Sn coils and support large Lorentz forces. The structure with the stainless-steel skin was selected as a baseline due to its relative simplicity and lower cost.

The maximum field for this magnet is limited to 15 T due to mechanical considerations. It was decided to perform the first magnet assembly with lower coil pre-load to achieve just 14 T and, in order to minimize the risk of coil damage during assembly and operation. This paper presents the design and fabrication details of the Nb_3Sn dipole demonstrator, called also MDPCT1 (Magnet Development Program Cos-Theta model 1), and reports the results of magnet training in the first test run. Results of magnetic measurements in this test run are discussed in [4]. Quench protection studies for this magnet are planned for the second test, following magnet reassembly with the nominal pre-load.

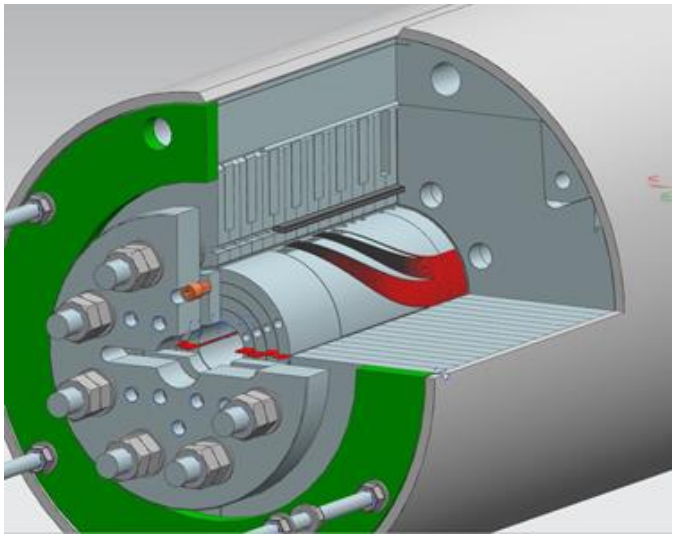

Fig. 1. 3D view of the magnet cold mass non-lead end.

II. Magnet Design and Construction

The details of the MDPCT1 design and the magnet design parameters are presented in [2]. The magnet consists of a 60-mm aperture 4-layer shell-type coil, graded between the inner and outer layers, a cold iron yoke, a thick stainless steel shell, and a coil axial support structure. Figure 1 shows the 3D view of MDPCT1 from the magnet non-lead end.

A. Strand and Cable

The cable in the two innermost layers has 28 strands 1.0 mm in diameter, whereas the cable in the two outermost layers has 40 strands 0.7 mm in diameter. Both cables were manufactured at Fermilab using RRP Nb_3Sn composite wires produced by Bruker-OST. The 0.7 mm RRP-108/127 wire and the 1.0 mm RRP-150/169 wire have sub-elements' size of 41 μm and 52 μm respectively to minimize the persistent current effect and

Manuscript received September 24, 2019. This work was supported by Fermi Research Alliance, LLC, under contract No. DE-AC02-07CH11359 with the U.S. Department and US-MDP.

E. Barzi, J. Carmichael, G. Chlachidze, V.V. Kashikhin, I. Novitski, S. Krave, C. Orozco, S. Stoynev, D. Turrioni, A.V. Zlobin are with FNAL, P.O. Box 500, Batavia, IL 60510, USA, (phone: 630-840-8192; fax: 630-840-8079, zlobin@fnal.gov).

S. Caspi is with LBNL.

D. Schoerling and D. Tommasini are with CERN.

Color versions of one or more of the figures in this paper are available online at http://ieeexplore.ieee.org.

Digital Object Identifier will be inserted here upon acceptance.

increase cable stability with respect to flux jumps. A 0.025-mm thick and 11-mm wide stainless steel strip was placed inside both cables to suppress the inter-strand eddy currents induced by the varying magnetic field in the coils. The cables were insulated with two layers of 0.075-mm thick and 12.7-mm wide E-glass tape.

The RRP strand and Rutherford cable cross-sections are shown in Fig. 2. The cross-section of both cables was optimized to minimize the strand critical current degradation [5]. The reaction cycles for both cables were optimized to achieve the highest possible J_c at the cable operation fields and preserve the copper matrix Residual Resistivity Ratio *(RRR)* [6].

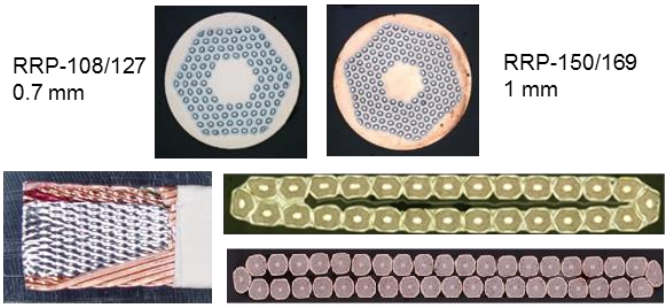

Fig. 2. Cross-sections of RRP strands (top), Rutherford cables (bottom right) and a view of the stainless-steel core inside the 28-strand cable (bottom left).

B. Coils

The 4-layer magnet coil consists of an inner coil and an outer coil. Each coil consists of two layers, and both layers were wound from a single piece of cable. The cable length in the inner coils is 73 m and in the outer coils 117 m. The inner coil poles were made of Ti-6Al-4V alloy and the wedges were made of a Glidcop alloy. The end spacers were made of stainless steel using the selective laser sintering (SLS) process. The outer coil poles and end parts were made of stainless steel. The materials for the coil components were sected using coil stress considerations. The cable layer jump in both coils is integrated into the lead end spacers.

The coil technology is based on the wind-and-react method, in which the superconducting Nb_3Sn phase is formed during the coil high-temperature heat treatment. After winding, coil layers were filled with CTD1202x liquid ceramic binder and cured under a small pressure at 150ºC for 0.5 hour. During curing the coil layers were shimmed to smaller azimuthal sizes than the nominal sizes to provide room for the cable expansion during reaction due to the Nb_3Sn phase formation [7]. Each coil was reacted in Argon atmosphere using an optimized 3-step cycles with T_{max}=669ºC for 50 hours for the inner coils (CL1) and T_{max}=658ºC for 48 hours for the outer coils (CL2).

To control the reproducibility of the coil reaction cycles and estimate the magnet short sample limits, 8 to 10 witness samples (strands extracted from the cable used in each coil) were reacted together with coils and then tested. The I_c values of the witness samples, measured at 15 T and 4.2 K for 3 inner coils and 3 outer coils, are shown in Fig. 3. There is good reproducibility of witness sample data for both inner and outer coils. The inner coil witness sample data are close to the target I_c and the outer coil witness sample data are slightly higher than the target I_c values. The *RRR*, measured using witness strands extracted from CL1 and CL2 cables was within 227-271 and 67-114 respectively, which is consistent with the expectations.

After reaction, the Nb_3Sn coil leads were spliced to flexible Nb-Ti cables. The coils were covered outside with two 0.040-mm thick layers of E-glass cloth and 0.05-mm thick Kapton layer with strip heaters and voltage taps in the middle, and inside with a 0.125 mm thick layer of E-glass cloth, impregnated with CTD101K epoxy and cured at 125°C for 21 hours.

The radial and azimuthal coil sizes were measured in the free condition in seven cross-sections along the length using a coordinate measuring machine. Smaller than nominal sizes were compensated by Kapton shims. Coil size variations along the coil straight sections were small, within ±30 μm, which did not require shim grading along the coil straight section. Pictures of the potted inner and outer coils with voltage taps and strip heaters on the coil outer surfaces are shown in Fig. 4.

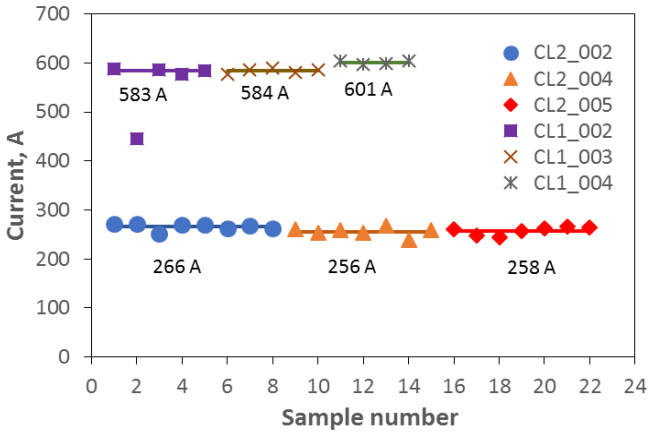

Fig. 3. Critical current of witness extracted strands at 15 T and 4.2 K.

Fig. 4. Inner (left) and outer (right) potted coils with instrumentation and additional strip heaters on the coil outer surfaces.

C. Magnet Assembly

Pictures of the main steps of the cold mass assembly are shown in Fig. 5. The coils were wrapped with 0.45 mm thick multi-layer Kapton ground insulation. Two main quench protection heaters, composed of 0.025 mm thick stainless steel strips, were placed inside the ground insulation on each coil side

with total Kapton insulation thickness on the coil side of 0.1 mm. The coil assembly, surrounded by 316L stainless steel and iron sheets each 2-mm thick, was installed inside the vertically-split iron yoke. The yoke is made of AISI 1020 iron laminations with an outer diameter of 587 mm, connected by strong 7075-T6 aluminum I-clamps, and surrounded by a 12.5-mm thick 316 stainless-steel skin. The coils were supported axially by two 50-mm thick end plates made of 304L stainless steel connected by 8 stainless steel rods 30 mm in diameter. To optimize the magnet mechanical structure and develop its assembly procedure, a short mechanical model and a full-size technological model were assembled and tested. The results of this work are summarized in [7]. The picture of the assembled MDPCT1 cold mass is shown in Fig. 6.

Fig. 5. The cold mass assembly steps: a) insertion of coil block inside the half-yoke; b) yoke clamping with I-clamps; c) insertion of clamped yoke inside the half-skin; d) cold mass inside tooling is moving to press for skin welding.

Fig. 6. Demonstrator dipole cold mass.

D. Coil Pre-load

The coil pre-load at room temperature is provided by the coil mid-plane and coil-yoke shims, the yoke-clamp interference, the yoke-skin shims and skin tension after welding. During and after magnet cool-down, the coil stress is controlled by the size of the vertical gap between the yoke blocks. The transverse mechanical rigidity of the structure is provided by the rigidity of the iron laminations, aluminum clamps and stainless steel skin [2], [8].

To minimize the risk of coil damage the first magnet assembly was done with lower coil pre-load, sufficient to achieve 14 T. The calculated distribution of the coil stress at different stages based on the coil stress measurements at 300 K is shown in Fig. 7. The coil stress in MDPCT1 is less than 150 MPa at all conditions. The coil-pole tension starts to develop after 13 T, increasing to 30 MPa at 14 T.

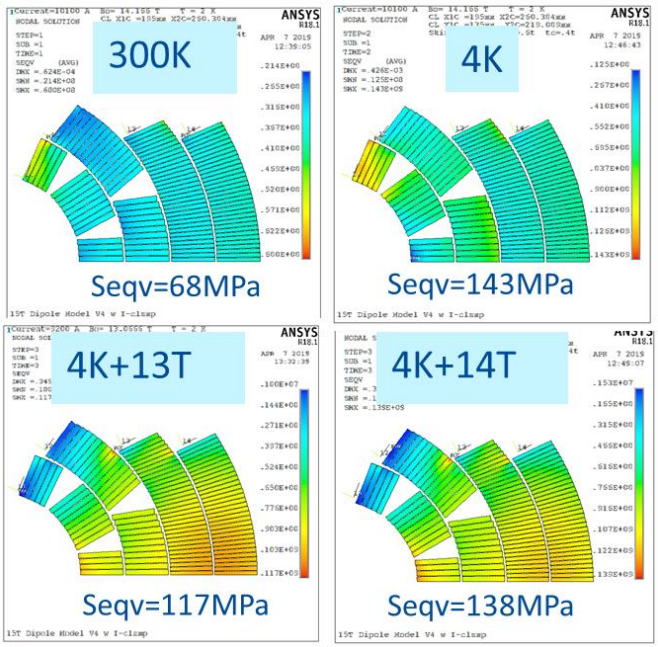

Fig. 7. Calculated distribution of the target pre-stress in the four magnet layers.

E. Magnet Parameters

The MDPCT1 parameters are summarized in Table 1. The magnet short sample limits were estimated based on the witness sample measurement data shown in Fig. 3.

TABLE 1:
MDPCT1 PARAMETERS

Parameter	Value
Magnet aperture	60 mm
Magnet outer diameter	612 mm
Geometrical length including splice box	1.46 m
Total magnet weight	2390 kg
Short sample bore field B_{ssl} at 4.5 K	15.2 T
Short sample bore field B_{ssl} at 1.9 K	16.8 T

III. TEST RESULTS

MDPCT1 was tested at Fermilab's Vertical Magnet Test Facility in June 2019. The first test results are reported in [9]. The magnet test program in the first test run was focused on the magnet training and magnetic measurements. All the inner and outer coils were equipped with voltage taps to record quenches and their location in a coil. To measure mechanical stresses in various elements of the structure, stain gauges were placed on

the inner coil surfaces, inner and outer coil pole pieces, end bullets, clamps and skin. Some elements of magnet instrumentation are seen in Figs. 4 and 6. Quench antennas, sensitive only to quenches in the innermost coil layer, were installed in the magnet aperture.

The magnet training was performed at 1.9 K to the target field of ~14 T. The final quench was made at 4.5 K. MDPCT1 quench history is plotted in Fig. 8. The first quench at 1.9 K was detected at a current of 7550 A, which corresponds to a field in the magnet bore of 11.3 T. After four quenches the magnet current reached ~9 kA (at a bore field slightly above 13 T) and the training rate slowed down. The target field of 14 T for this test was achieved after 11 quenches, after which the magnet reached its quench plateau. Then, the magnet was warmed up to 4.5 K and quenched again. This last quench was at 9742 A, which corresponds to a bore field of 14.112 T, based on the 3D calculations, and 14.13±0.02 T based on the magnet *B/I* measurements [4]. This was the highest bore field reached in this test run.

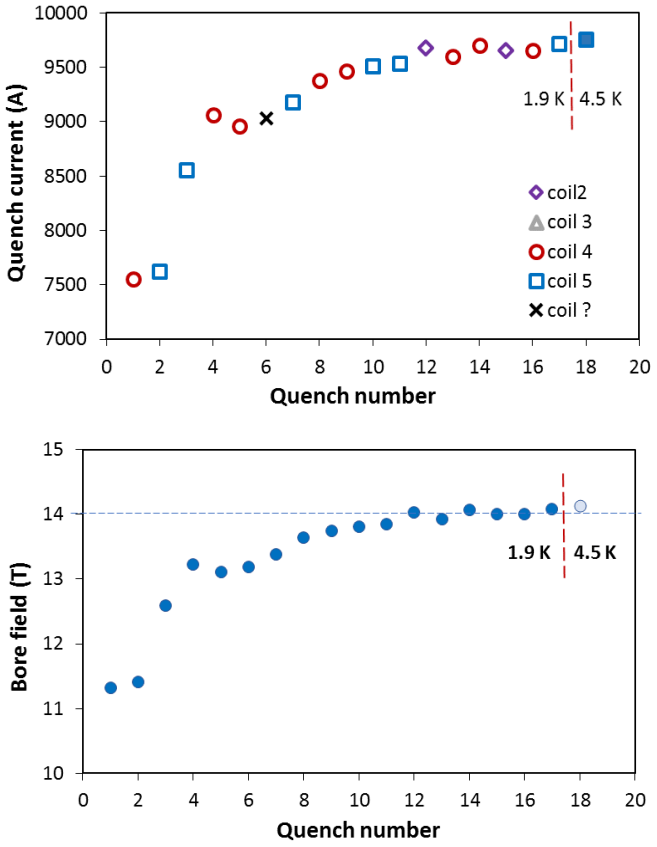

Fig. 8. Quench current (top) and quench bore field (bottom) vs. quench number for MDPCT1.

Most of the quenches were detected in outer coils 4 and 5. The location of quench #6 was not identified. The training performance of coil 4 and 5 is quite similar. The quenches were almost equally distributed between the two outer coils and were seen in both layers. The more precise localization of quench origin in the outer coils was not possible due to damage of the coil instrumentation traces. Only two quenches, #12 and #15, were detected in inner coil 2, whereas no quenches were detected in inner coil 3.

Quench field B_q at 1.9 K and 4.5 K, normalized to the magnet short sample bore field B_{ssl} at the same temperature, vs. quench number is shown in Fig. 9. The magnet training started at 67% of the B_{ssl} at 1.9 K, and the maximum quench current at 1.9 K was at 83% of the B_{ssl} at this temperature. At 4.5 K the magnet reached 93% of its B_{ssl} and 94% of its ultimate design field of 15 T.

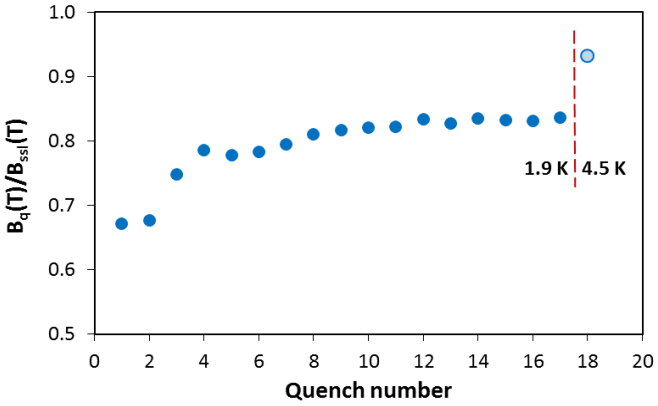

Fig. 9. Normalized quench bore field vs. the quench number.

The *RRR* values, measured for MDPCT1, are 249 and 259 for the two inner coils, and 81 and 95 for the two outer coils. These numbers are in a good agreement with the corresponding witness sample measurements. The resistances of splices between the Nb_3Sn coil leads and the Nb-Ti cables, measured in the current range of 2 to 9 kA, are within 0.3-0.8 nOhm.

IV. Conclusion

The Nb_3Sn dipole demonstrator MDPCT1 for a post-LHC hadron collider was developed and tested. This work is an important MDP milestone to understand the limits of Nb_3Sn accelerator magnet technology. The graded 4-layer coil design, the innovative support structure and the magnet fabrication procedure were tested. Whereas the maximum field for this design is 15 T due to mechanical concerns, for the first test the magnet was assembled with lower coil pre-load sufficient to achieve 14 T and minimize the risk of coil damage during assembly and operation.

The goals of the first test have been achieved. After a short training at 1.9 K, MDPCT1 reached 14.1 T at 4.5 K or 94% of its design limit, setting a new world record for accelerator magnets at 4.5 K. The magnet training was stopped at this point. It will continue after the magnet re-assembly to increase the coil azimuthal pre-load to a level sufficient to achieve the goal of 15 T, and to improve the axial support of the coils. The magnet second test is planned for February 2020.

Acknowledgment

The authors thank technical staff of FNAL, LBNL and CERN for contributions to the magnet design, fabrication and test, and the US-MDP Management Group and Technical Advisory Committee for the support of this project. Special thanks to A. Rusy. J. Karambis and S. Johnson for their valuable contributions to the magnet assembly and production tests.

REFERENCES

[1] A.V. Zlobin et al., "Design concept and parameters of a 15 T Nb_3Sn dipole demonstrator for a 100 TeV hadron collider", Proc. of IPAC2015, Richmond, VA, USA, p.3365.

[2] I. Novitski et al., "Development of a 15 T Nb_3Sn Accelerator Dipole Demonstrator at Fermilab", IEEE Trans. on Appl. Supercond., Vol. 26, Issue 3, June 2016, 4001007.

[3] I. Novitski, A.V. Zlobin, "Development and Comparison of Mechanical Structures for FNAL 15 T Nb_3Sn Dipole Demonstrator", ISBN 978-3-95450-180-9, Proc. of NAPAC2016, Chicago, IL, USA, p.137.

[4] T. Strauss et al., "First Field Measurements of the 15 T Nb_3Sn Dipole Demonstrator MDPCT1", *this conference.*

[5] E. Barzi et al., "Nb_3Sn RRP® Strand and Rutherford Cable Development for a 15 T Dipole Demonstrator," IEEE Trans. on Appl. Supercond., Vol. 26, Issue 3, June 2016, 4001007.

[6] E. Barzi et al., "Heat Treatment Optimization of Rutherford Cables for a 15 T Nb_3Sn Dipole Demonstrator", IEEE Trans. on Appl. Supercond., Vol. 27, Issue 4, June 2017, 4802905.

[7] C. Orozco et al., "Assembly and Tests of Mechanical Models of the 15 T Nb_3Sn Dipole Demonstrator," IEEE Trans. on Appl. Supercond., Vol. 29, Issue 5, August 2019, 4003404.

[8] C. Kokkinos et al., "FEA Model and Mechanical Analysis of the Nb_3Sn 15 T Dipole Demonstrator," IEEE Trans. on Appl. Supercond., Vol. 28, Issue 3, April 2018, 4007406.

[9] A.V. Zlobin et al., "Quench performance and field quality of the 15 T Nb_3Sn dipole demonstrator MDPCT1 in the first test run", Proc. of NAPAC2019, Lansing (MI), 1-6 September 2019, paper MOPLO20.